Report on the in-flight vignetting calibration of the MOS cameras aboard the XMM NEWTON satellite

Doris M. Neumann
CEA/SACLAY SAp, France

The observations of G21.5

To determine the effect of vignetting we used the observations of the supernova remnant G21.5. In total G21.5 was observed five times with XMM-Newton. One on-axis observation (on CCD1 in revolution 60) and four off-axis observations with each an off-axis angle of about 10 arc minutes. In the off-axis exposures G21.5 was observed with MOS1 (MOS2) on CCD6 (CCD2) (revolution 61), CCD5 (CCD6) (revolution 62), CCD3 (CCD5) (revolution 64) and CCD2 (CCD3) (revolution 65) – see also Fig.1. The four off-axis pointings were necessary to determine the spatial influence of the reflection grating array (RGA) through which the photons pass. About half the photons are dispersed onto the RGS, the other half is transmitted onto the MOS cameras.

Data reduction

Our data reduction is based on the SAS.

Ignoring time intervals with high background level

In order to enhance the signal-to-noise ratio we excluded time intervals of high background. A typical light curve of the G21.5 observations is displayed in Fig.2. We only select time intervals with less than 26 counts per 2.6sec into account (2.6sec is the frame time of the MOS cameras). We did not select in a specific energy band.

Region selection

In some of the off-axis pointings G21.5 lies very close to the border of the exposed CCD's. In order to avoid photon loss due to edge effects, which might bias downwards our measured counts, we consider only the counts of the source in an aperture with a radius of $40''$. – A cut well below the distance of the source to the CCD gap.

Estimating PSF-effects

The XMM-Newton telescopes have a point-spread function (PSF) which varies across the field-of-view and which broadens in outer regions. In order to see whether this effect has some

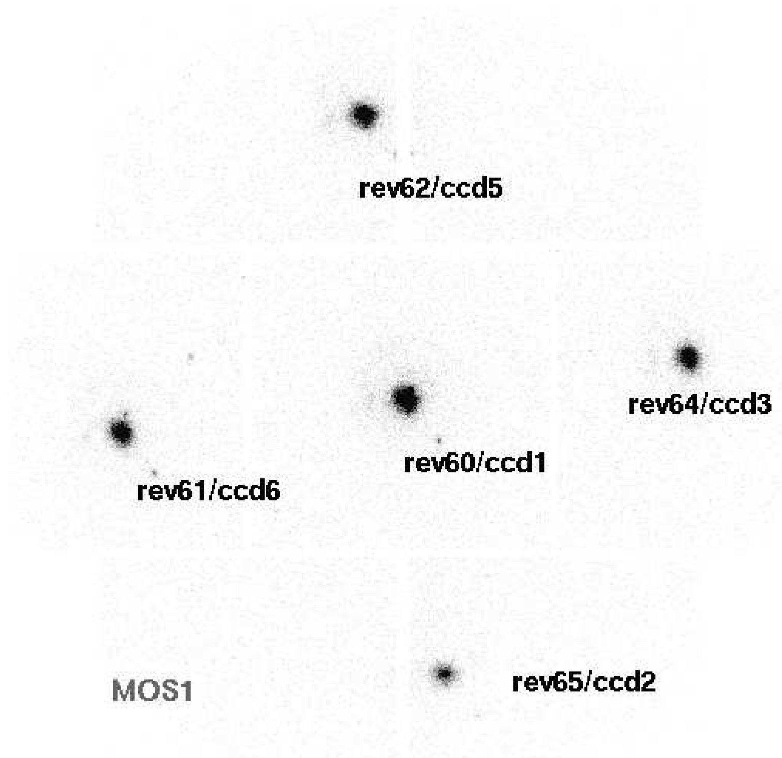

Figure 1: The pointing positions of G21.5 on the different CCD's for the MOS1 camera. For MOS2 the positions are rotated 90 degrees anti-clockwise

measurable influence on the vignetting study on G21.5 with our aperture, we convolve the data of the source in the on-axis pointing with the off-axis PSF at 10 arcmin. The change of the count rate within our defined aperture is in the order of less than 1 per cent. The error is well within our statistical errors and we therefore neglect the broadening of the PSF in the following.

Energy binning

As the effect of vignetting due to the telescopes is expected to be energy dependent we divided the data of G21.5 into eight energy bands: 0.5–2.0 keV, 2.0–2.5 keV, 2.5–3.0 keV,3.0–4.0 keV, 4.0–5.0 keV, 5.0–6.0 keV, 6.0–8.0 keV and 8.0–10.0 keV. The widening of the chosen energy bands towards higher energies is necessary to account for the loss of sensibility of the mirror/detector combination. We left out the low energy band (0.1–0.5 keV) due to remaining uncertainties in the flat fielding of the CCD's in this energy range. – Above 0.5 keV there are no observed differences in spatial sensibility across the CCD's (J.L. Sauvageot, E. Belsole, private communication).

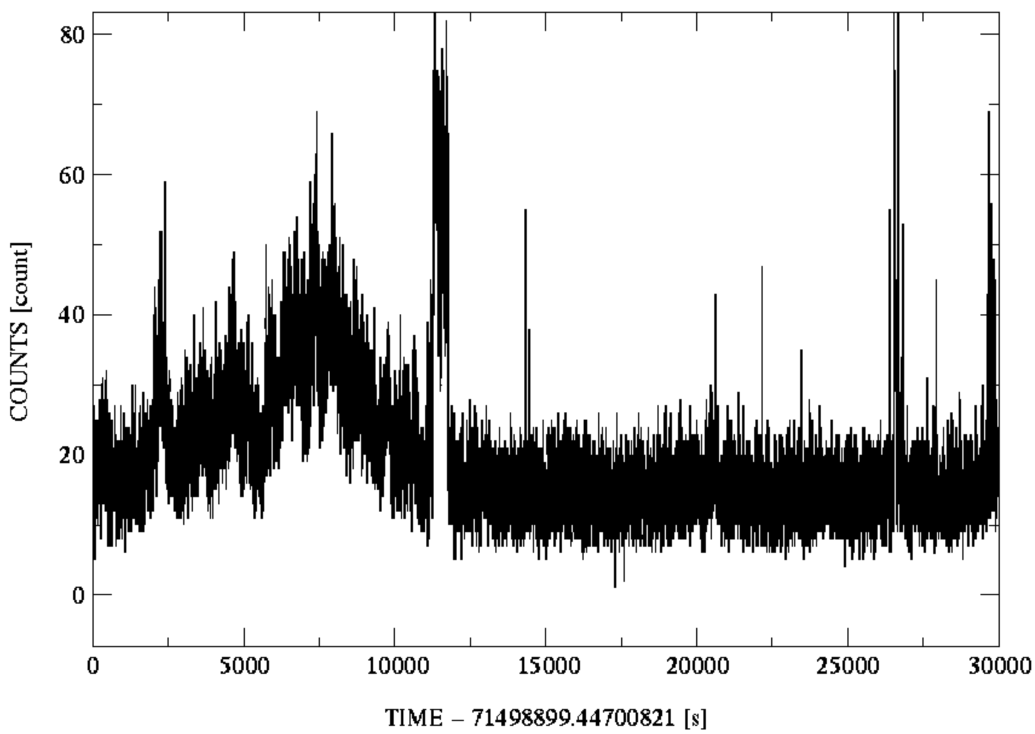

Figure 2: The light curve of the on-axis pointing of G21.5 for the MOS2 camera. The binning of the times is 2.6sec, conforming the frame time of the MOS cameras.

Background determination and statistical error handling

For the vignetting study we count the photons in each energy band in the on-axis and the off-axis pointing. We subtract the background contribution, which we measure by determining the mean count rate per pixel in an annulus around the source ($150'' < r < 200''$). For the background determination we only include the region of the annulus which coincides with the CCD on which G21.5 was observed. The ratio of off-axis/on-axis count rates can be seen in Fig.4 and Fig.5. The uncertainty estimates are based on Poisson statistics coming from the measured source (on-axis and off-axis) and background counts.

Comparison with various on-ground vignetting calibrations

Fig.3 shows the ratio off-axis/on-axis counts, or vignetting factor corrected for background as a function of energy for MOS1 for all offset pointing positions of G21.5. The ratios are corrected for the different useful exposure times of the pointings, which range between 11 and 21 ksec. In Fig.3 we also plot different curves coming from ground-based calibration.

As we can see, the flight measurements based on G21.5 are in relatively good agreement with the predictions of the telescope coming from old calibration files (red curve in Fig.3), currently available on the XMM home-page (`http://xmm.vilspa.esa.es/user/calib_top.html`). The scatter around this line can be explained by the influence of the RGA. The calibration files deduced from the CCF in the SAS (black curve in Fig.3) ALWAYS underestimate the vignetting significantly.

The calibration files on the XMM home-page date from a time before the mirrors were actually built (information from P. Gondoin). The CCF results in the SAS in principle include the calibration of the mirrors and are much more recent.

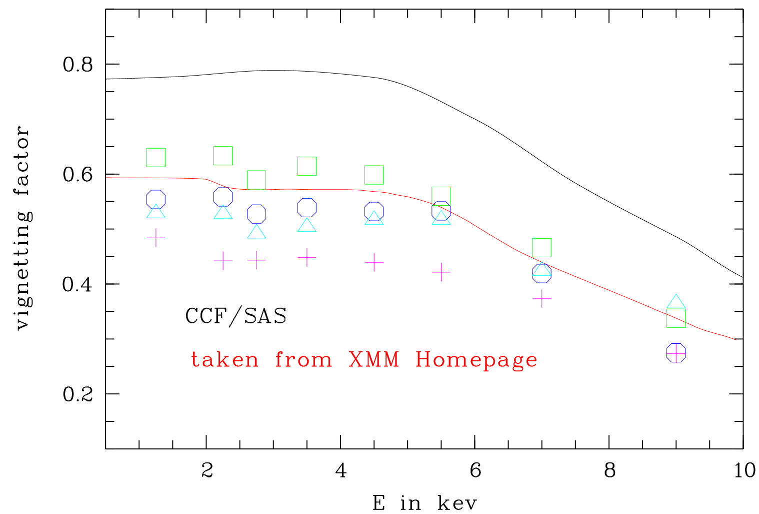

Figure 3: The vignetting factor defined as ratio of off-axis versus on-axis counts of the G21.5 MOS1 observations as function of energy. The off-axis pointings lie 10 arcminutes away from the optical axis (see also Fig.1). The black and red curve come from ground-based measurements. The black curve represents the result of the CCF in the SAS. The red curve comes from the calibration files from the XMM homepage (see also text).

The spatial variations of transmission of the RGA

As predicted we see that the RGA seems to influence the vignetting. However, this influence seems to be independent of energy. Fig.4 shows the vignetting curves for the different positions for MOS1, and Fig.5 for MOS2, respectively. Again, the vignetting curves account for the different exposure times of the observations. We see, as predicted, that there is more transmission from the RGA in the upper part of the detector than in the lower part in the case of MOS1. However, it seems that the predictions including the RGA are somewhat above the measured points. This indicates that the effect of the vignetting is underestimated. Furthermore, in the case of camera MOS1 it seems that the DETY-dependence (DETY for y-direction in detector coordinates) of the RGA is not linearly but that it is less important in the upper part of the camera (CCD5) than in the lower part (CCD2). However, we want to stress that this finding might be also only an effect of vignetting, which was not properly accounted for.

For MOS2, while writing this report, it was not clear to the author what spatial dependence to take in the case of the MOS2 camera. The results of the analysis based on G21.5 indicate that a simple rotation by 90 degrees with respect to camera MOS1 (camera MOS1 and MOS2 are rotated by 90 degrees) is not sufficient. This is clearly still an open issue.

Furthermore to check whether gain variations from CCD to CCD might play an important role we performed, for MOS2, the vignetting study on PHA and on PI channels (up to now we only looked at PI channels). The gain represents the conversion from PHA to PI channels. The latter ones are corrected for detector effects and are in 'real photon energies'.

Systematic errors in the gain might introduce some bias in the vignetting study, since the predefined energy bands (in PI channels) might be falsely identified. As we can see, the analysis based on PHA is relatively similar to PI. However, it seems that the vignetting in this case shows a stronger dependence on energy. The differences for the vignetting between PI and PHA can be explained by the fact that the gain for each CCD is slightly different (see also CCF).

Comparison with other XMM NEWTON observations

Our results for the vignetting, including RGA effects, are also in agreement with a similar vignetting study which we performed on the galaxy cluster Abell 496, which was also observed at several positions with XMM NEWTON. However, this study was somewhat limited to lower energies due to the softer spectrum of this source in comparison with G21.5. In addition, due to the large extend, which covers the whole field-of-view, background determination is a problem. The background had to be measured far away from the cluster center, which might introduce some bias in the measurements.

Our results are also in agreement with an analysis based on XMM data of Abell 1795, led by M. Arnaud, in which the surface brightness profiles obtained with the MOS cameras were compared with the brightness profile deduced from ROSAT/PSPC data. (See also: `ftp://epic3.xra.le.ac.uk/pub/cal-pv/meetings/leicester-2000-07-025`). The vignetting and background corrected ROSAT profiles were shallower at radii larger than 10 arcminutes than the vignetting and background corrected profiles from the XMM MOS cameras (the vignetting correction was based on both calibration files, the one from the XMM home-page, the other one from the SAS CCF's. The correction was performed by S. Majerowicz). The difference between ROSAT and XMM profiles corrected with the SAS CCF's was larger than the difference between ROSAT and XMM profile based on the home-page calibration file. This indicates, again, that the vignetting effect is underestimated, much more though for the SAS CCF files than for the home-page files.

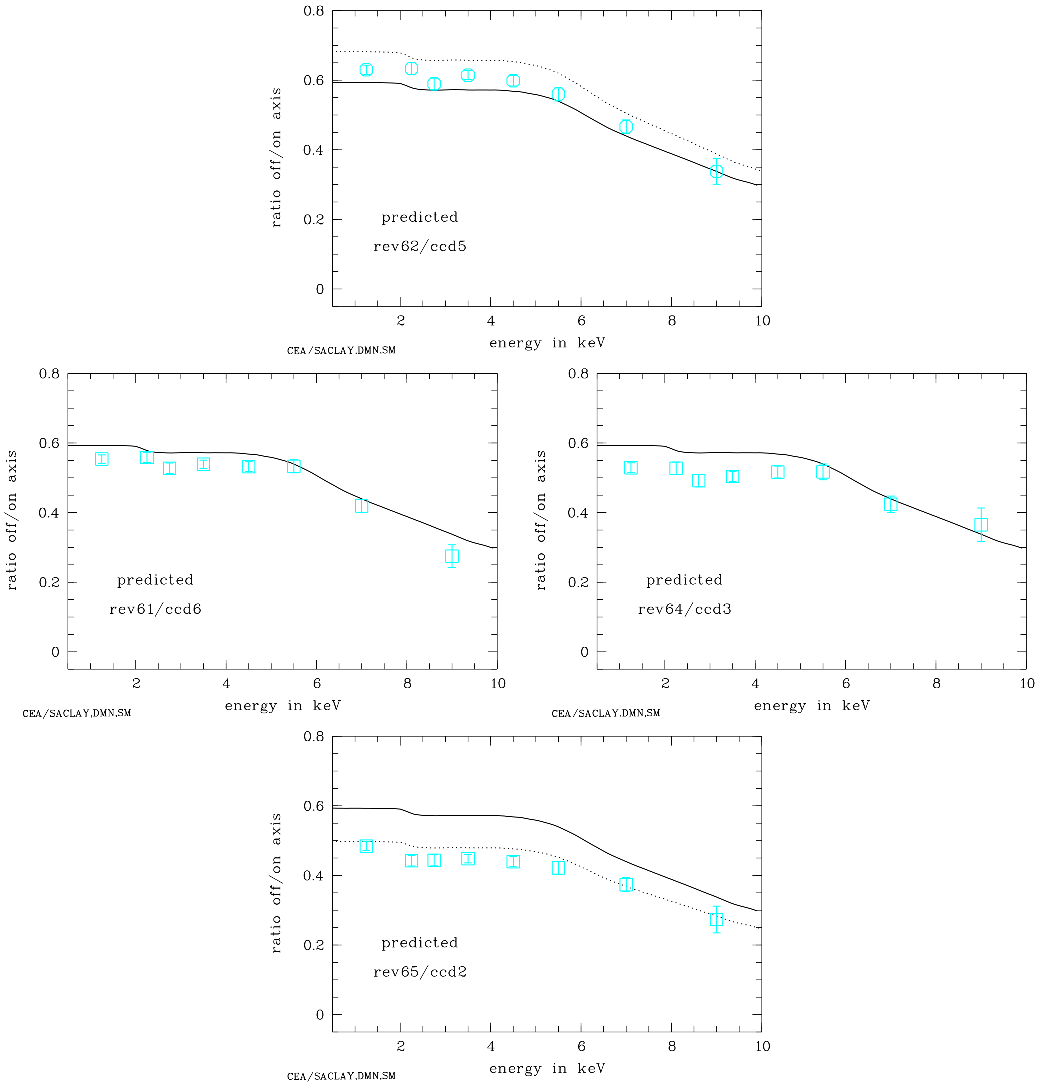

Figure 4: The vignetting factor for the MOS1 camera for different CCD's. The full line represents the vignetting of the telescope alone (from XMM home-page). The dashed line shows, additionally, the predicted dependence of the RGA (source: P. Gondoin). The location of the graphs corresponds to the different positions of the CCD's on the camera.

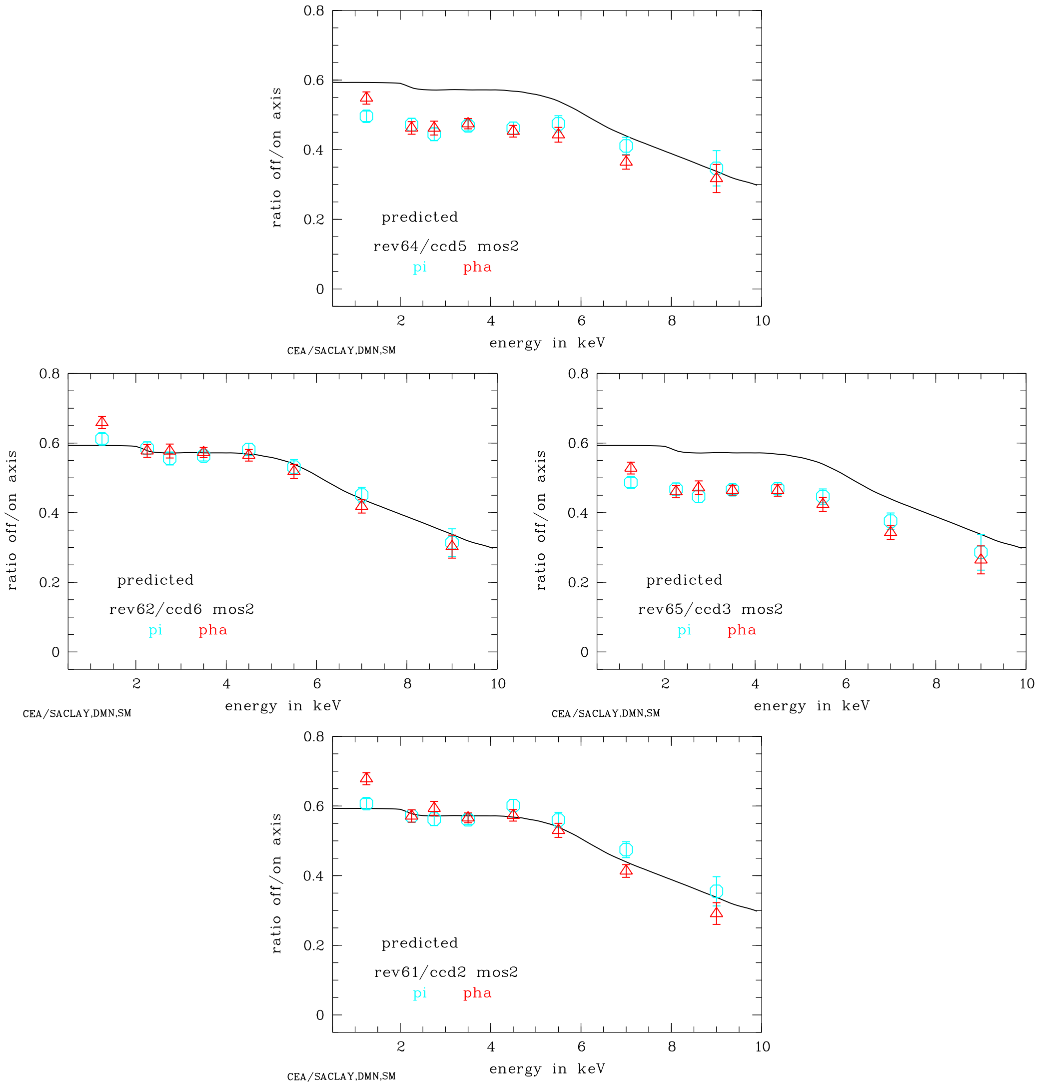

Figure 5: The vignetting factor for the MOS2 camera for different CCD's. The full line represents the vignetting of the telescope alone (from XMM home-page). At the moment of writing this report it was not clear to the author what orientation to take for the RGA dependence. In order to see what possible gain variations can do we determined the energies and subsequent vignetting factors using the PI (blue circles) and the PHA channels (red triangles). The location of the graphs corresponds to the different positions of the CCD's on the camera.

Conclusions

We performed a vignetting study based on the XMM NEWTON MOS observations of G21.5. We find:

- The vignetting of the telescopes versus off-axis angle for different energy bands is relatively well described by the files from the XMM home-page (`http://xmm.vilspa.esa.es/user/calib_top.html`). It seems that there is still some small under-prediction of the vignetting in these files.
- The calibration files in the SAS greatly under-predict the effect of vignetting (typically by a factor of about 30%).
- There is indeed some spatial dependence of the RGA observable for MOS1 and MOS2. For MOS1 it seems to be a one-dimensional dependence in DETY-direction. For MOS2 we do not yet know from the observational point of you.- Some input from people at ESA is necessary here.
- It seems that the spatial dependence of the RGA in the case of MOS1 is not linear but shows some sort of flattening at the high transmission end (at high DETY values). However, this flattening might also be caused by a general under prediction of the vignetting.

Open issues / questions / inconsistencies

- Why do the old files from the XMM home-page, which only include theoretical aspects of the mirror fit better the actual in-flight data of G21.5 than the SAS CCF files, which are more recent and include the ground-based calibration?
- Is the spatial dependence of the RGA transmission only a one-dimensional function (like a function of DETY for MOS1) and is it linear?
- What is the orientation for the spatial dependence of the RGA in MOS2?
- Is it easy to have access to the calibration files of EACH INDIVIDUAL instrument and not only the effects of different instruments at the same time? (like RGA spatial dependence alone?)
- Do we expect important modifications in the SAS, which might alter our results on the vignetting? (for example different gains of the different CCD's)

Miscellaneous

This report might be subject to modification. D. Lumb and C. Erd indicated that the CCF files will be modified. As soon as these modifications are available they will be included in the report.

Acknowledgments

I want to thank J. Ballet for essential SAS support. I am very grateful for the help of R. Gastaud and S. Majerowicz for preparing the calibration files. I thank P. Gondoin, D. Lumb and C. Erd for discussions and the fact that they provided necessary calibration files. I am also grateful for the discussions with M. Arnaud.